Volume 15, Number 2, 2022. pp. 161-168

Jordan Journal of Physics

ARTICLE

X-Wave Propagation Characteristics in a Collisional, Inhomogeneous Plasma Slab

Manal M. Al-Ali

Department of Physics, Yarmouk University, Irbid, Jordan.

Doi: **https://doi.org/10.47011/15.2.6**

Received on: 17/10/2020; Accepted on: 26/01/2021

Abstract: Normally incident electromagnetic wave on a collisional, inhomogeneous magnetoplasma slab has been treated as a multilayered system of homogeneous sub-cells within the transfer matrix method. For incident wave frequencies much above the ion cyclotron frequency, the extraordinary elliptically polarized wave mode is relevant for wave propagation normal to a dc-magnetic field. For a sinusoidal plasma density profile, the transmittance, reflectance and absorbance are plotted *versus* wave frequency normalized to electron cyclotron frequency ω_0 / ω_{ce} for different ratios of electron cyclotron to electron plasma frequencies. For fixed ω_{ce} and by varying the wave frequency, the curves of the transmittance and reflectance show two pass and two stop bands. When the ratio of cyclotron frequency to plasma frequency $\omega_{ce} / \omega_{pc}$ is increased, all bands shift to the region of low wave frequency, the pass bands become broader and the stop bands become narrower. The absorbance show three absorption bands; namely, two collisional absorption bands of evanescent waves at the X-wave cut-off frequencies and a resonance absorption band at the upper hybrid frequency. It has also been found that a homogeneous plasma slab overestimates the collisional absorption at cut-offs and has a broader absorption band of the upper hybrid resonance.

Keywords: Waves in inhomogeneous magnetoplasma, Upper hybrid resonance, Reflectance, Absorbance, Transmittance.

I. Introduction

Scattering, interaction and propagation of electromagnetic waves in a magnetoplasma have been attracting many researchers [1-10] due to the wide range of applications that includes, but is not limited to, atmospheric and space plasma, stealth plasma, telecommunications, fabricated industrial absorbers and filters, as well as other applications.

Due to their unique electrical and dynamical properties, plasmas support a wide range of plasma oscillations and waves. The importance of waves in plasmas as non-perturbing diagnostic, probing and exciting tools, makes plasma waves one of the active sub--disciplines in plasma physics research [11-15]. Of practical and theoretical interest are the classification, understanding and characterization of linear and/or nonlinear waves in different regimes of plasma.

Owing to its wide range of variables, a plasma slab can be especially engineered and its parameters controlled in a way to tailor the material with the attempted optical properties to serve the intended application. By interacting with the tailored slab, the electromagnetic wave properties are then studied and the effect of the different plasma parameters on the reflection, absorption and transmission of the EM--wave is discussed.

Corresponding Author: Manal M. Al-Ali **Email**: manal.alali@yu.edu.jo

Gurel and Oncu [3] studied the interaction of EM-waves with a strongly collisional plasma slab of partially linear and partially sinusoidal density profile and found that highly collisional and high-density plasma greatly absorbs the electromagnetic wave power along a wide frequency band.

AL-Khateeb et al. [8] used the forward recursion approach to study the characteristics of EM-wave perpendicular propagation in a collisional plasma slab in the GHz range for a set of parameters that may suit reentry blackout. The forward recursion method showed results that are consistent with those shown in the literature using the scattering matrix method qualitatively and qualitatively. Laroussi [16] and Hu [17] used the scattering matrix method to obtain reflectance, absorbance and transmittance of EM-waves in an inhomogeneous plasma slab.

In this work, inhomogeneous magnetoplasma with a sinusoidal plasma density profile is considered. The magnetoplasma will be treated as a multilayered system of homogeneous sub-slabs within the Max-Born transfer matrix technique [10, 18, 19]. The present work is a continuation of the work published recently by Rawwaqa et al. [10], where they studied the characteristics of waves propagating along the ambient magnetic field resulting in right and left circularly polarized waves (R-waves and L-waves). The present study, however, treats the case of wave propagation normal to an externally applied magnetic field with the wave modes supported by the magnetoplasma being of extraordinary nature (X-waves) with elliptical polarization. The X-waves have a completely different nature from that of the R-wave and L-wave in terms of resonance and cut-off behaviors that affect magnitude, morphology and intervals of reflection, absorption and transmission. The paper is organized as follows: In Section II, we present the model equations. Numerical results are presented in Section III. Finally, in section IV, we discuss the main results and conclusions.

II. Model Equations

Fig. 1 shows the geometry of the plasma slab, where we assume that waves are normally incident from the left semi-infinite medium into the bound plasma slab of width a. The dielectric permittivity of left and right semi-infinite regions are ϵ_ℓ and ϵ_r, respectively.

Assume an incident linearly polarized plane wave in the *y*-direction such that $\vec{E}(\mathrm{z,t}) = \hat{y}E_y(\mathrm{z,t})$ and the incident, reflected and transmitted waves are propagating along the *x*-axis perpendicular to a background uniform magnetostatic field $\vec{\mathrm{B}} = \hat{z}B_0$, as shown in Fig. 1. As the wave propagates into the magnetoplasma slab, it induces an electric field E_x along $\vec{k}$ and thus becomes partly longitudinal and partly transverse. Wave modes in a magnetoplasma slab with the induced electric field being normal to the dc-magnetic field tend to be elliptically polarized [12-14].

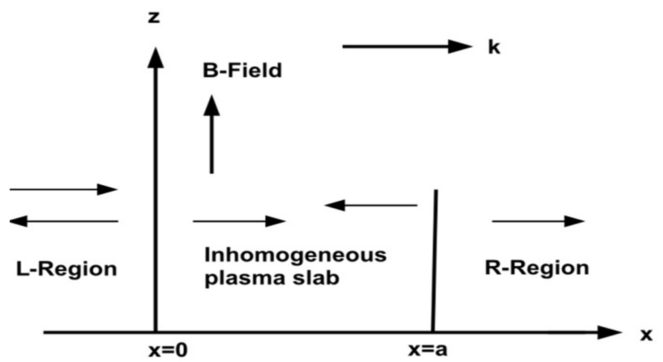

FIG. 1. Bound inhomogeneous plasma slab in a dc-magnetic field.

The inhomogeneous plasma slab is divided into N sufficiently thin homogeneous layers of width $d_{m+1} - d_m$, where $m = 1,2,3,......,N$ [10, 18, 20]. The electromagnetic fields at the inner face of the exit layer $m = N$ are related to the fields at the input interface of incidence by the well-established global transfer matrix M of the whole multilayered structure; namely,

$$M = \prod_{m=1}^{N} M_m = \begin{pmatrix} M_{11} & M_{12} \\ M_{21} & M_{22} \end{pmatrix}, \qquad (1)$$

$$M_m = \begin{pmatrix} \cos\delta_m & \frac{\mathrm{i}}{\gamma_m}\sin\delta_m \\ \mathrm{i}\gamma_m \sin\delta_m & \cos\delta_m \end{pmatrix}, \qquad (2)$$

where M_m stands for the mth layer transfer matrix. The parameters γ_m and δ_m for normal incidence are as follows:

$$\gamma_m = \sqrt{\mu_m \epsilon_m} = \sqrt{\mu_0 \epsilon_0}\sqrt{\varepsilon_m}\ ,\ \delta_m = \omega d_m \gamma_m\ , \qquad (3)$$

where ω is the angular frequency of the incident wave, μ_m, ϵ_m, d_m and ε_m are, respectively, the mth layer permeability, permittivity, width and dielectric function. All necessary information to characterize the propagation of electromagnetic waves across the inhomogeneous plasma slab is contained in Eqs. (1-3). The complex transmission $\tilde{\tau}$ and reflection $\tilde{\rho}$ coefficients in terms of global transfer matrix elements are [18, 20]:

$$\tilde{\tau} = \frac{2\gamma_\ell}{\gamma_\ell M_{11} + \gamma_\ell \gamma_r M_{12} + M_{21} + \gamma_r M_{22}}\ , \qquad (4)$$

$$\tilde{\rho} = \frac{\gamma_\ell M_{11} + \gamma_\ell \gamma_r M_{12} - M_{21} - \gamma_r M_{22}}{\gamma_\ell M_{11} + \gamma_\ell \gamma_r M_{12} + M_{21} + \gamma_r M_{22}}. \qquad (5)$$

The corresponding reflectance R and transmittance T are obtained as $R = \tilde{\rho}\tilde{\rho}^*$ and $T = \sqrt{\frac{\varepsilon_r}{\varepsilon_\ell}}\tilde{\tau}\tilde{\tau}^*$. The absorbance (A) is defined as $A = 1 - R - T$.

III. Numerical Results

We assume a sinusoidal plasma density which is appropriate for ionospheric applications such that $n_e(\mathrm{x}) = \mathrm{n}_{0e}\sin\frac{\pi x}{a}$ for $0 \le x \le \frac{a}{2}$ and $n_e(\mathrm{x}) = \mathrm{n}_{0e}[1 - \sin\frac{\pi}{a}(\mathrm{x} - \frac{a}{2})]$ for $\frac{a}{2} \le x \le a$, where n_{0e} is the peak density of plasma electrons. For wave propagation perpendicular to the applied magnetic field, a magnetoplasma of cold electrons and cold immobile ions supports both ordinary (O) and extraordinary (X) transverse electromagnetic wave modes. Since the ordinary wave is unaffected by the magnetic field, only the X-wave will be considered [22-24].

The *X*-wave has two pass bands in the frequency ranges $\omega_L < \omega < \omega_{uh}$ and $\omega > \omega_R$ which are separated by a stop band in the frequency range $\omega_{uh} < \omega < \omega_R$. Here, ω_{pe} is the electron plasma frequency, ω_{uh} is the upper hybrid frequency, ω_L and ω_R are, respectively, the left and right cut-off frequencies of the X-wave [12]-[14]. They are given by the following formulae;

$$\omega_{uh} = \sqrt{\omega_{pe}^2 + \omega_{ce}^2}\ ,\ \omega_{pe} = \sqrt{\frac{e^2 n_e}{\epsilon_0 m_e}}\ , \qquad (6)$$

$$\omega_L = \frac{1}{2}\sqrt{\omega_{ce}^2 + 4\omega_{pe}^2} - \frac{\omega_{ce}}{2}\ , \qquad (7)$$

$$\omega_R = \frac{1}{2}\sqrt{\omega_{ce}^2 + 4\omega_{pe}^2} + \frac{\omega_{ce}}{2}\ . \qquad (8)$$

The m^{th} layer dielectric function for the X-wave is given by [21]:

$$\varepsilon_X^{(m)} = \frac{[1 - \frac{\omega_{pe,m}^2}{\omega(\omega - \omega_{ce,m} - j\nu_{e,m})}][1 - \frac{\omega_{pe,m}^2}{\omega(\omega + \omega_{ce,m} - j\nu_{e,m})}]}{1 - \frac{\omega - j\nu_{e,m}}{\omega}\frac{\omega_{pe,m}^2}{(\omega - j\nu_{e,m})^2 - \omega_{ce,m}^2}}, \qquad (9)$$

where $\omega_{ce,m}$ and $\nu_{e,m}$ are the electron plasma frequency and the collision frequency with neutrals of the m^{th} sub-slab, respectively.

In all numerical examples presented below, we use normalized quantities and therefore, we initiate the calculations by an arbitrary incident wave frequency $\omega = \omega_0$. In all calculations to follow, we adopt the normalized width of the plasma slab $a/\lambda_0 = 5$. The normalized electron plasma frequency in each plasma slab can take one of the values $\omega_{pe}/\omega_{ce} = 1/\sqrt{2}, 1, \sqrt{2}$. The normalized collision frequency of electrons with neutrals has a fixed ratio of $\nu_e/\omega_{pe} = 0.01$, which accounts for weak, but relevant, collisional damping.

To characterize the X-wave propagation in an inhomogeneous magnetoplasma slab, we use the ratio ω_0/ω_{ce} as an independent variable. Accordingly, the magnetic field increases by moving to the left at fixed wave frequency ω_0 or the wave frequency increases as we move to the right at a fixed value of the dc-magnetic field.

In Figs. 2-4, we plot the reflectance, transmittance and absorbance *versus* ω_0 / ω_{ce} for three different plasma frequencies. For each fixed value of the cyclotron frequency and by varying the wave frequency ω_0, the curves of Figs. 2 and 3 show two pass and two stop bands. The pass bands are in the frequency ranges $\omega_L < \omega_o < \omega_{uh}$ and $\omega_0 > \omega_R$, and the corresponding stop bands are such that $0 < \omega_o < \omega_L$ and $\omega_{uh} < \omega_o < \omega_R$.

With increasing the ratio $\omega_{ce} / \omega_{pe}$, all bands are shifted to the left. The pass bands of the transmittance become broader (Fig. 2), while the corresponding stop bands of the reflectance become narrower (Fig. 3). We observe the same behavior in the absorbance curves of Fig. 4. The absorbance curves show the appearance of three absorption bands. From left to right, the first and third bands of each curve are due to collisional absorption of evanescent waves at the cut-off frequencies $\omega_0 = \omega_L$ and $\omega_0 = \omega_R$, respectively. The second (middle) absorption band is due to upper hybrid resonance which is localized around ω_{ce}.

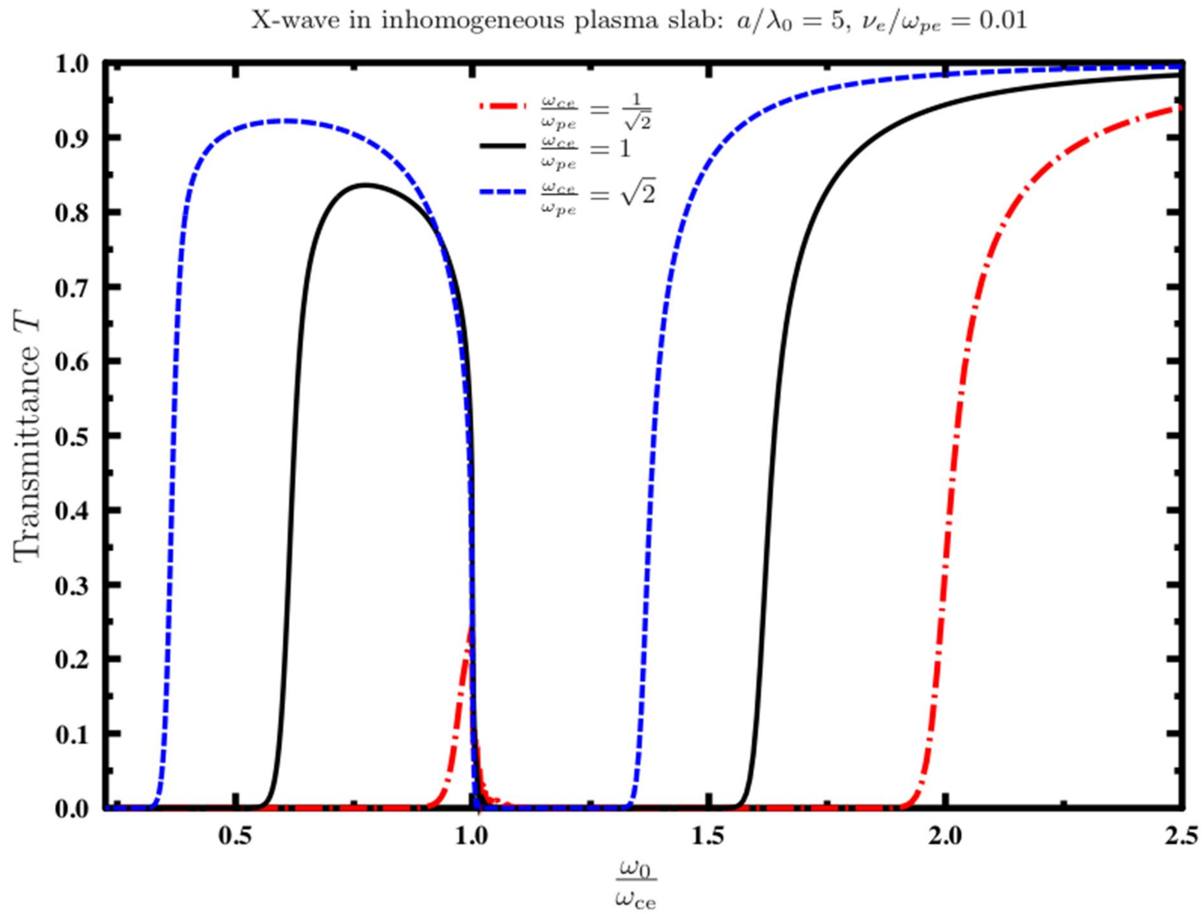

FIG. 2. Transmittance for inhomogeneous magnetoplasma slab.

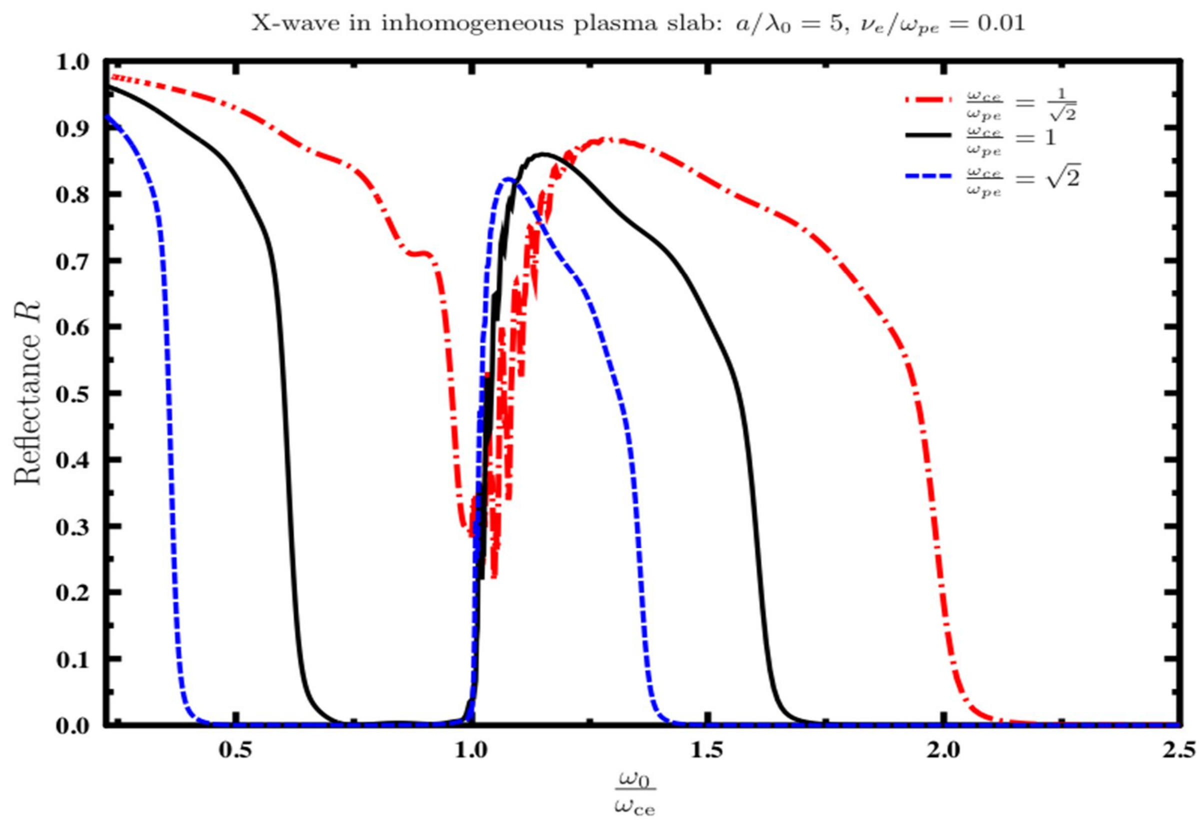

FIG. 3. Reflectance for inhomogeneous magnetoplasma slab.

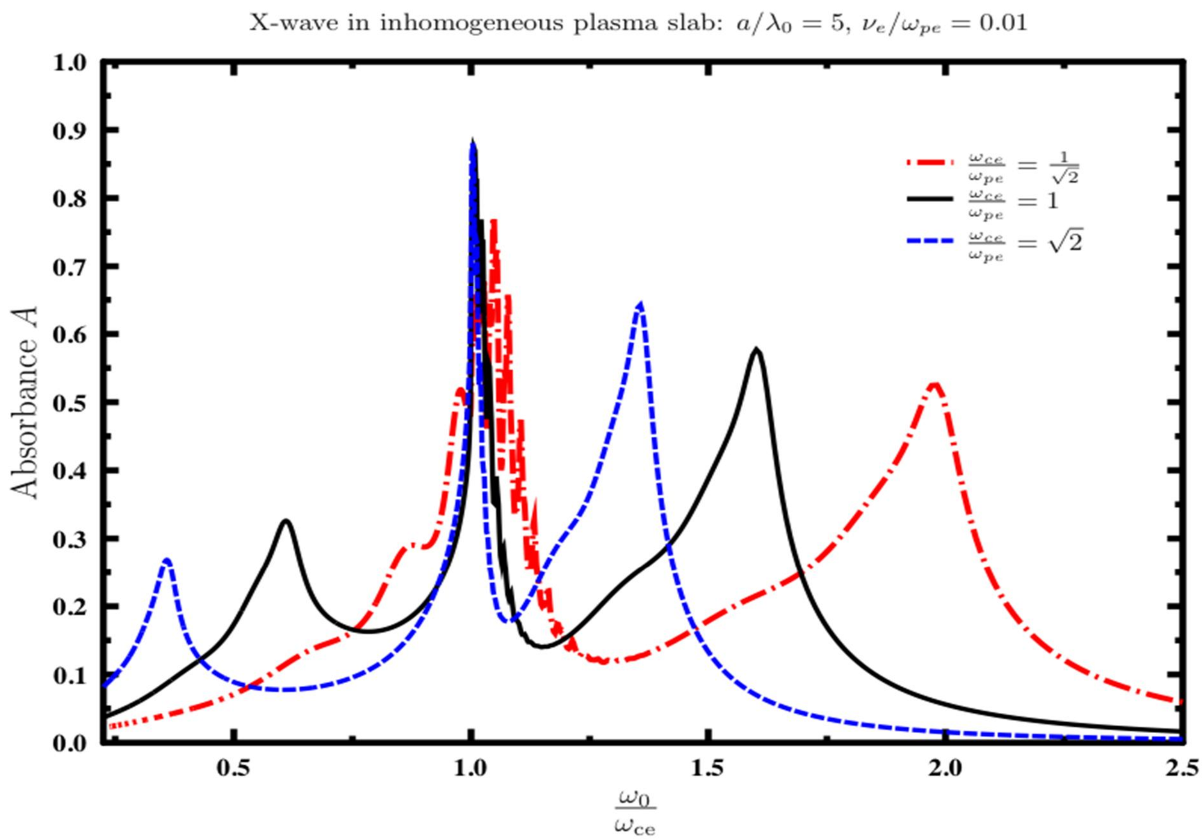

FIG.4: Absorbance for inhomogeneous magnetoplasma slab.

To complete the discussion on the X-wave propagation characteristics in an inhomogeneous magnetoplasma slab of finite thickness, we plot in Figs. 5 and 6 the curves of R and A for homogeneous and inhomogeneous magnetoplasma slabs. We observe from Fig. 5 that the stop band $\omega_{uh} < \omega_o < \omega_R$ is narrower for a homogeneous slab, while the second stop band $0 \leq \omega_o < \omega_L$ is broader. The ripples in curves of R for the homogeneous plasma slab are of geometrical nature and are due to the in-plasma interferences. The ripples in R are smeared out for an inhomogeneous plasma slab.

The absorbance curves of Fig. 6 show the appearance of three absorption bands for the homogeneous plasma slab. These absorption bands are due to the collisional absorption of evanescent waves and to the upper hybrid resonance. We observe that the effect of inhomogeneity is to down shift the absorption (and the stop) bands to the left toward lower wave frequencies. From Fig. 6, we see that a homogeneous plasma slab overestimates collisional absorption at cut-offs and broadens the upper hybrid resonance absorption band.

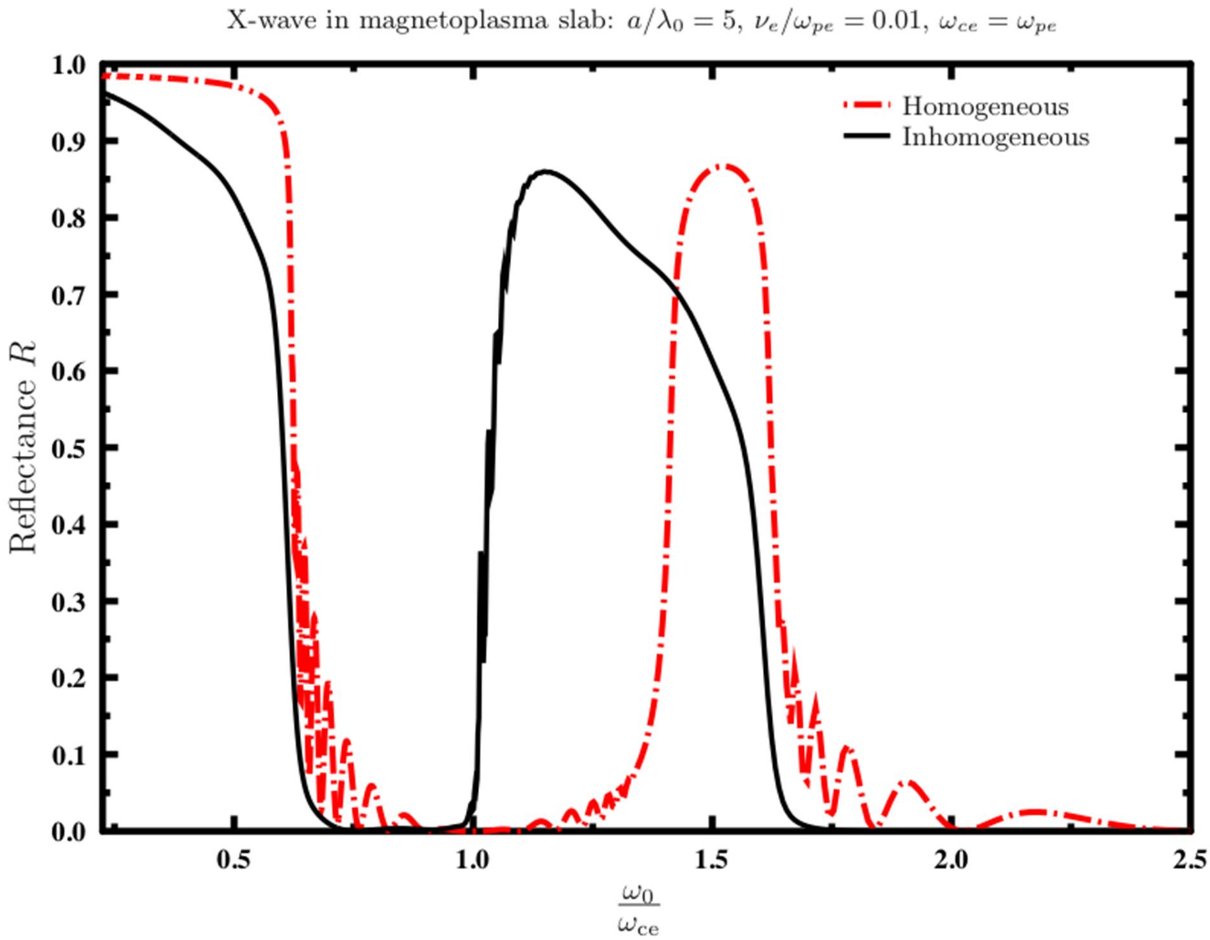

FIG. 5. Reflectance for homogeneous and inhomogeneous magnetoplasma slabs.

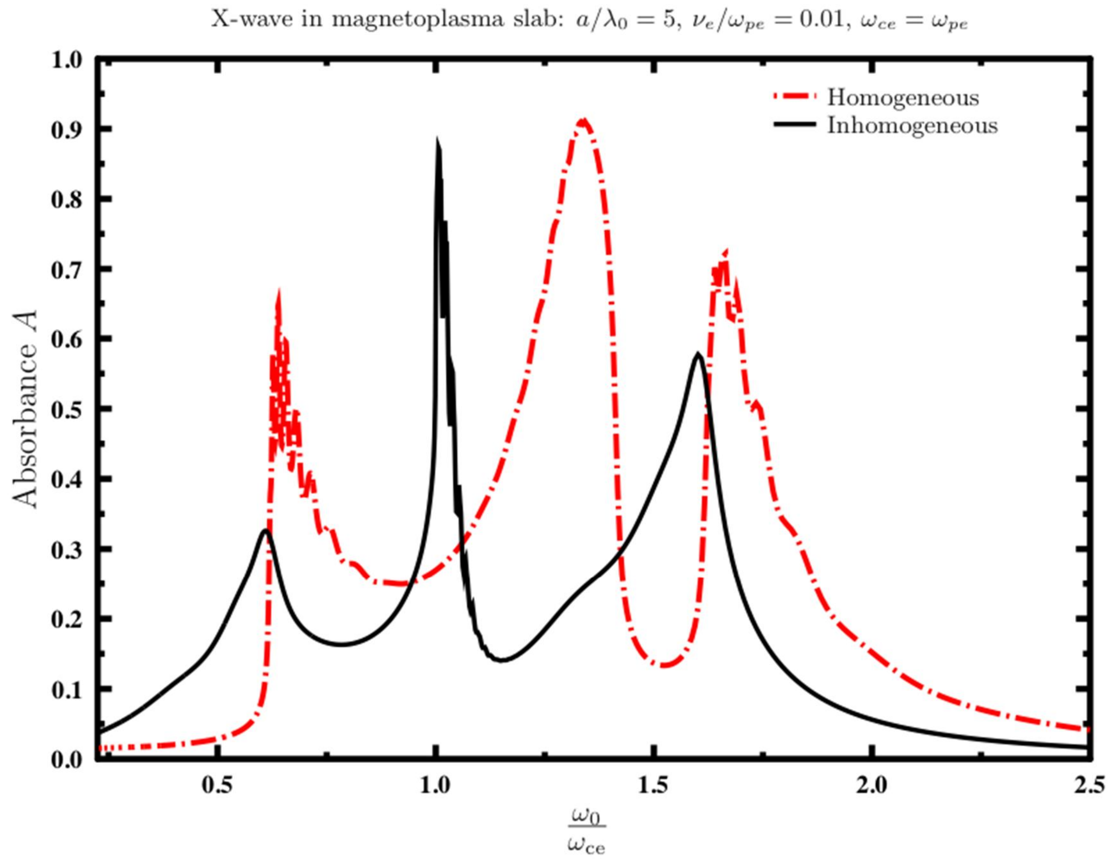

FIG. 6. Absorbance for homogeneous and inhomogeneous magnetoplasma slabs.

IV. Conclusion

In this paper, we investigate the propagation characteristics of a normally incident electromagnetic wave on a cold, weakly collisional and inhomogeneous magnetoplasma slab. Within the transfer matrix technique and for sinusoidal plasma density profile, the inhomogeneous slab is treated as a multilayered system of homogeneous sub-slabs. We only considered electron motion for wave frequencies much above the ion cyclotron frequency. For wave propagation perpendicular to a static magnetic field, only the elliptically polarized extraordinary wave is coupled to the electrons.

In Figures 2-6, the transmittance, reflectance and absorbance are plotted *versus* ω_0/ω_{ce} for different ratios of cyclotron to plasma frequencies. By varying the wave frequency ω_0 for fixed ω_{ce}, the curves of transmittance and reflectance show two pass and two stop bands. When the ratio ω_{ce}/ω_{pe} is increased, the bands shift to the region of low wave frequency, the pass bands become broader and the stop bands become narrower.

Curves of the absorbance show three absorption bands. The first and third bands (from left to right) of each curve are collisional absorption bands of evanescent waves at the cut-off frequencies ω_L and ω_R, respectively. The middle absorption band is due to the upper hybrid resonance.

X-wave propagation characteristics in an inhomogeneous magnetoplasma slab of finite thickness have been compared with those of a homogeneous plasma slab. The stop band $\omega_{uh} < \omega_0 < \omega_R$ for a homogeneous slab is narrower, while the stop band $0 < \omega_0 < \omega_L$ is broader. The ripples in the reflectance curves for the homogeneous slab due to in-plasma interferences are washed out by inhomogeneity. The effect of the inhomogeneity on the absorbance curves of Fig.6 is to down shift the absorption (and the stop) bands to the left toward lower wave frequencies.

A homogeneous plasma slab overestimates a collisional absorption at cut-offs and broadens the upper hybrid resonance absorption band.

References

[1] Sharma, S.R., Canadian Journal of Physics, 44 (1966) 255.

[2] Zhang, J., Fu, H. and Scales, W., IEEE Transactions on Plasma Science, 46 (2018) 2146.

[3] Gurel, C.S. and Oncu, E., Progress in Electromagnetics Research Letters, 12 (2009) 171.

[4] Bawa'aneh, M.S., Al-Khateeb, A.M. and Sawalha, A.S., Canadian Journal of Physics, 90 (2012) 241.

[5] Bawa'aneh, M.S., Al-Khateeb, A.M. and Sawalha, A.S., IEEE Transactions on Plasma Science, 41 (2013) 2496.

[6] Bawa'aneh, M. S., Al-Khateeb, A.M. and Ghim, Y.-C., IEEE Transactions on Antennas and Propagation, 66 (2018) 6525.

[7] Chen, X.-Y., Shen, F.-F., Liu, Y.-M., Ai, W. and Li, X.-P., IEEE Trans. Plasma Sci., 46 (2018) 1755.

[8] Al-Khateeb, A.M., Khasawneh, M.A. and Bawa'aneh, M.S., Advanced Electromagnetics, 8 (2019) 44.

[9] Mori, T., Nishiura, M., Yoshida, Z. and Kenmochi, N., Plasma and Fusion Research, 14 (2019) 3401134.

[10] Rawwaqa, F., Al-Ali, M.M., Al-Khateeb, A.M. and Bawa'aneh, M.S., Advanced Electromagnetics, 9 (2020) 25.

[11] Daqa, W.M., Al-Khateeb, A.M., Al-Sharif, A.I. and Laham, N.M., Jordan J. Phys., 1 (2008) 9.

[12] Chen, F.F., "Introduction to Plasma Physics and Controlled Fusion", 2nd Edn., (Plenum, New York, 1984).

[13] Stix, T.H., "Waves in Plasmas", (AIP, New York, 1992).

[14] Swanson, D.G., "Plasma Waves", 2nd Edn., (IOP Publishing, Ltd, 2003).

[15] Hutchinson, I.H., "Plasma Diagnostics", 2nd Edn., (Cambridge University Press, 2002).

[16] Laroussi, M. and Roth, J.R., IEEE Trans. Plasma Sci., 21 (1993) 366.

[17] Hu, B.J., Wei, G. and Lai, S.L., IEEE Transactions on Plasma Science, 27 (1999) 1131.

[18] Born, M. and Wolf, E., "Principles of Optics: Electromagnetic Theory of Propagation, Interference and Diffraction of Light", 7th Edn., (Cambridge University Press, 2003).

[19] Budden, K.G., "Radio Waves in the Ionosphere", (Cambridge University Press, 1961).

[20] Pedrotti, F.L., Pedrotti, L.M. and Pedrotti, L.S., "Introduction to Optics", 3rd Edn., (Cambridge University Press, 2017).

[21] Lieberman, M.A. and Lichtenberg, A.J., "Principles of Plasma Discharges and Materials Processing", 2nd Edn., (John Wiley & Sons, Inc., Hoboken, New Jersey, 2005).

[22] Bawa'aneh, M.S., Contributions to Plasma Physics, 43 (2003) 447.

[23] Bawa'aneh, M.S., Journal of Plasma Physics, 72 (2006) 687.

[24] Bawa'aneh, M.S. and Boyd, T.J.M., Journal of Plasma Physics, 73 (2007) 159.